Discontinuous basalt and glass fiber reinforced PP composites from textile prefabricates: effects of interfacial modification on the mechanical performance

Czigany T., Deak T., Tamas P.

Accepted for publication in Composite Interfaces
Published in 2008
DOI: 10.1163/156855408786778302

Composite Interfaces, Vol. 15, No. 7–9, pp. 697–707 (2008)

Also available online - www.brill.nl/ci

Discontinuous basalt and glass fiber reinforced PP composites from textile prefabricates: effects of interfacial modification on the mechanical performance

T. CZIGÁNY *, T. DEÁK and P. TAMÁS

Department of Polymer Engineering, Faculty of Mechanical Engineering, Budapest University of Technology and Economics, H-1111 Budapest, Műegyetem rkp. 3, Hungary

Received 24 January 2008; accepted 10 March 2008

Abstract—Spun and blown basalt fibers and their PP matrix composites were investigated. The composites were manufactured by hot pressing technology from carded and needle punched prefabricate using PP fiber as matrix material. Glass and blown basalt fibers were treated with reaction product of maleic acid-anhydride and sunflower oil while spun basalt fibers had a surface coating of silane coupling agent. Fibers were investigated with tensile tests while composites were subjected to static and dynamic mechanical tests. The results show that blown basalt fibers have relatively poor mechanical properties, while spun basalt fibers are comparable with glass fibers regarding geometry and mechanical performance. The static and dynamic mechanical properties of glass and spun basalt fiber reinforced composites are similar and are higher than blown basalt fiber reinforced composites. Results were supported with SEM micrographs.

Keywords: Basalt fiber; polymer composites; mechanical properties; reactive surfactants.

1. INTRODUCTION

Polymer composites are nowadays typically reinforced by glass, carbon, aramid or natural fibers such as flax, sisal, hemp or wood fibers. Recently a new type of fiber produced from volcanic rock by melt technology has come to the front — the basalt fiber [1]. Basalt can be found on the surface of the Earth's crust (containing 40–60% SiO_2), and these fibers exhibit a number of excellent properties. In addition to their high modulus and excellent heat resistance, basalt fibers are good electric insulators, biologically inactive and environmentally friendly [2, 3].

The most important components of basalt are SiO_2, Al_2O_3, CaO, MgO, Fe_2O_3 and FeO [4, 5]. Its structure and chemical composition are similar to those of

*To whom correspondence should be addressed. E-mail: czigany@eik.bme.hu

glass. Its color ranges from brown to dark green. It is molten between 1350 and 1700°C and its average density is 2.7 g/cm^3. When cooled rapidly, it solidifies in a glassy amorphous phase. Slower cooling results in a partially crystalline structure. Basalt materials are classified according to their SiO_2 content as alkaline basalts (up to 42% SiO_2), mildly acid basalts (43–46% SiO_2) and acid basalts (over 46% SiO_2). Basalt fibers are more resistant to strong alkalis than glass fibers, but glass can better withstand strong acids [6–9]. For continuous fiber manufacturing, basalt rocks must meet the following requirements: SiO_2 content above 46% (acid basalt) with constant composition, ability to melt without solid residue, appropriate melt viscosity for fiber formation and ability to solidify in a glassy phase without noticeable crystallization [3].

Basalt fibers are typically produced by two different technologies [10]. The so-called blowing technology with centrifugal cylinders (e.g. Junkers method) is used for manufacturing cheap fibers with 60–100 mm length and 8–20 μm diameter, primarily used as insulating materials in the construction and automotive industries [11, 12]. For more demanding applications continuous fibers, which can be processed by textile technologies, are prepared by spinneret technology from the melt — similarly to traditional glass fiber production. These continuous fibers of 10–14 μm diameter can be obtained in the form of rovings containing different numbers of elementary fibers. Short fibers can be produced directly from crushed basalt stones and the technology is very simple so the fibers are very cheap, but they have relatively poor and uneven mechanical properties. An important application of basalt fibers is the substitution for asbestos, e.g. in car brake pads, due to its high temperature resistance [13]. The first continuous basalt fibers of adequate quality were produced with experimental equipment in 1963 in Ukraine. Today the production of continuous basalt fibers is concentrated in the former Soviet Union. The most notable production companies are Kamenny Vek (Russia) and Technobasalt (Ukraine). The raw material cost of basalt fiber is ≈1% of the corrresponding glass cost. Even so, continuous basalt fibers are not yet cheaper than glass fibers, due to the relatively high energy consumption and complexity of production. However, rapidly increasing production capacity will probably produce a price decline for continuous basalt fibers [14]. Generally, continuous basalt fibers are considered as a material that can fill the gap between glass fibers on the one hand and high performance but expensive fibers such as aramid and carbon on the other. In contrast with this, short basalt fibers are much cheaper than continuous ones. So far, basalt fibers have been investigated extensively by themselves and as reinforcement for thermoset matrix composites, but they have been scarcely applied for thermoplastic matrices [15–17].

The usage of basalt fibers as reinforcement of polymer composites is dynamically spreading [18–20], so the aim of this study is to compare the mechanical properties of different basalt fibers, and to introduce their polypropylene composites.

2. MATERIALS AND METHODS

Two different basalt fibers (BFs) were investigated: short basalt fiber, produced by melt blowing Junkers technology (Toplan Ltd., Hungary) (BF-B), and chopped continuous basalt fiber, produced by spinneret technology (Kamenny Vek, Russia) (BF-S). The average length of short basalt fibers was 60 mm. The properties of the basalt fibers were compared with TH5000-126 type glass fiber (GF) (Skoplast, Slovakia). The matrix material was polypropylene (PP) available in the form of fibers (Geo Tipptex Ltd., Hungary, type: TIPPFIL H 483 F, $MFI_{230°C/2.16\ kg} = 5$ g/10 min, average diameter: 34.3 ± 4.2 μm).

Spun continuous basalt fibers get a surface coating during production. The composition and characteristics of this coating are closely related with the production technology, which means that the application of a different coupling agent would require the removal of original sizing and formation of a new one; this in turn means an additional technology step. On the other hand, continuous basalt fibers are hard to handle and vulnerable without coating. This would make the additional treatment of continuous basalt fibers expensive and difficult; thus it was omitted in our study. Glass and short basalt fibers come without surface coating, so the coupling agent can be applied without preliminary technology steps. Thus continuous basalt fibers were used as received, with a sizing containing silane based coupling agents, optimized for epoxy matrix. BF-B and glass fibers were treated with the product of the addition reaction of sunflower oil (SFO) and maleic acid-anhydride (MA).

The mechanical properties of reinforcing fibers under static longitudinal loading were investigated by tensile tests. The diameter was measured on a Projectina 4014/BK-2 projection microscope fitted to an image processing system and equipped with a CCD camera, with 400× magnification. The diameters of fibers were measured at three different points to determine the variations in diameter. The tests were executed according to the JIS R 7601 standard, with 25 mm gauge length. The test speed was $v = 2$ mm/min. One hundred specimens of each material were tested and the mean values and standard deviations were calculated.

The composites were produced in a pressing technique from a pre-fabricate. Glass and continuous basalt (BF-S) fibers were chopped to a length of 60 mm for carding. PP fibers that served as the matrix material and acted also as carrying fibers (BEFAMA 3K type multi-cylinder carding machine) were fed into the machine together with the basalt and glass fibers. The nominal fiber content was 30 mass percentage (m%) in each case. The carded pre-fabricates were needle punched and as a result became more consistent and contained less air inclusions. Three millimeter thick plates were produced from the materials prepared in the way mentioned above with pressing on a Schwabenthan Polystat 300S type pressing machine, at the temperature of 200°C and pressure of 20 bar. The manufacturing process can be seen in Fig. 1.

Blown basalt (BF-B) fibers (Fig. 2) and glass fibers were sized in order to improve their interfacial adhesion with the PP matrix. This was carried out using reactive surfactants. They were treated with the addition reaction product of maleic

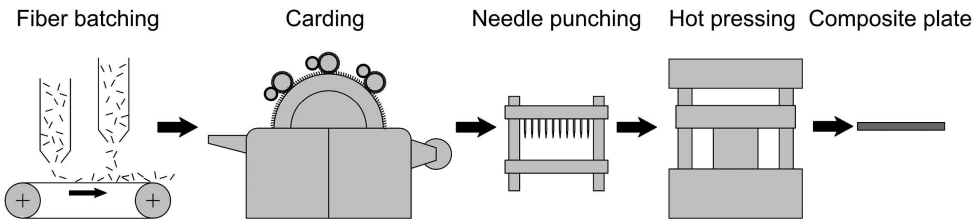

Figure 1. Manufacturing process of composite plates.

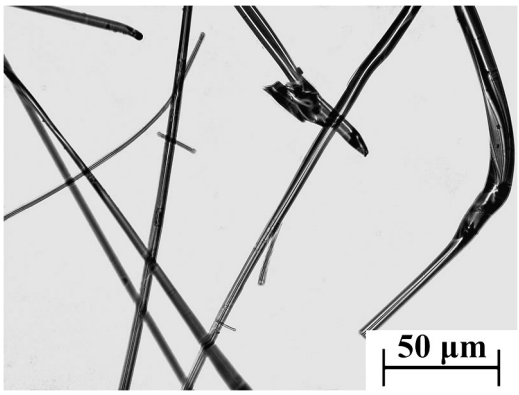

Figure 2. Optical micrograph of blown basalt fibers (BF-B).

acid-anhydride and sunflower oil, because according to literature data maleic acid treatment promotes interaction in most fiber reinforced systems. The principle of the reactive surfactant treatment is the following: molecules which simultaneously contain C=C bond, long carbon chain and reactive functional group, can be used effectively as adhesion promoter additive because, due to the C=C bond, they can be bonded to the PP molecule through a radical addition reaction. The long carbon chain gives them a wetting and dispersing effect; thus they concentrate on the phase boundary where subsequently they establish chemical and physical interactions. They develop strong interactions with the polar phase (the surface of reinforcing fiber in our case) by means of reactive functional groups (e.g. acid anhydride, carboxyl). The above conditions are not realized in the case of maleic acid-anhydride and unsaturated carboxylic acids. The application of maleic acid-anhydride as adhesion promoter additive is rather difficult, because it is very volatile at elevated temperatures, flammable, and it emits toxic vapors, while oleic acid has restrained functionality but it is not sufficiently reactive. However, molecules produced by Diels–Alder type esterification reaction or addition reaction of maleic acid-anhydride and carboxylic acids with high carbon atom content and their derivatives fulfill these requirements. The principle of Diels–Alder reactions is the following: the partial saturation of a conjugated system can be reached with a molecule containing an olefinic bond with adequate activity. Therefore the 9,11-linoleic acid and the glycerol-ester of linoleic acid (e.g. sunflower oil) react

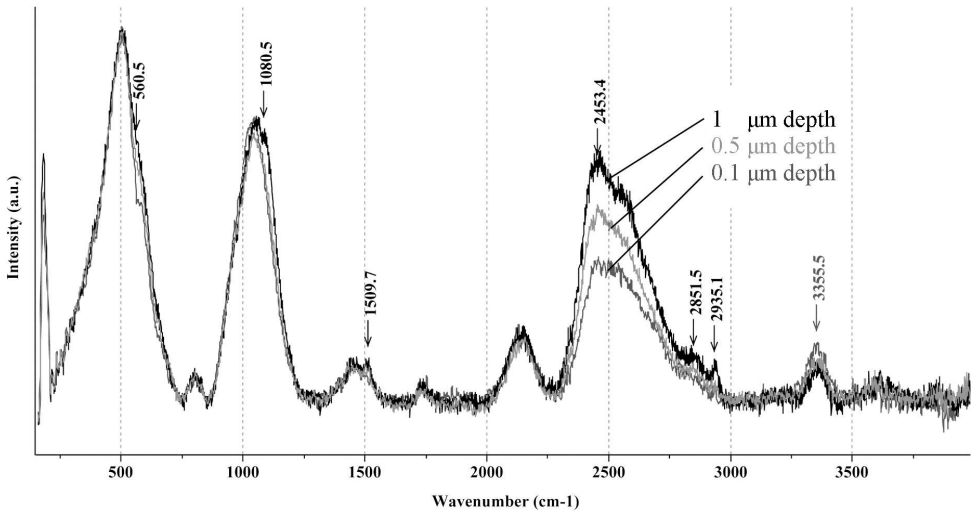

Figure 3. Raman spectroscopic analysis of glass fiber surface.

with the maleic acid-anhydride in the course of the formation of a six-membered ring. According to the above, the Diels–Alder adduct of sunflower oil (NFO) and maleic acid-anhydride was developed (NFO-MA). Sunflower oil is composed of triglycerides of different unsaturated fatty acids (22–39% of oleic acid, 26–34% of 9,11-linoleic acid, and 26–34% of 9,12-linoleic acid) and 5–7% of saturated fatty acids. As the distribution of fatty acids is uniform in natural glycerides, sunflower oil is predominantly built up from molecules that contain one of three unsaturated fatty acids.

NFO (density: 0.924–0.926 g/cm^3 (15°C), freezing point: −17°C, saponification number: 188–193, iodine number: 129–136, index of refraction: 1.4659–1.4721 (40°C)) (89.98 g) and MA (Sigma Chemical Co., USA, density: 1.5 g/cm^3, melting point: 52.8°C, sublimating, water soluble) (10.00 g) were fed into a flask equipped with a distiller head, in a molar ratio of 1:1. A few milligrams of hydroquinone were added in order to avoid the polymerization of sunflower oil due to high temperature and the presence of free radicals. The mixture was intensively stirred and gradually heated to 100–110°C in oil bath and vacuum. The temperature was held for 1.5 h. Figure 3 shows a schematic formula of the reaction product.

The fibers were coated with the sizing agent during the production of the carded pre-fabricate. The reaction mixture of sunflower oil and maleic acid-anhydride was sprayed on the carded mat coming down from the carding machine, in a ratio of 1 m% (correlated to the fiber content).

In order to investigate the static mechanical properties of the composites, the specimens were cut from the 3 mm thick pressed PP and composite laminates in both transverse (T) and longitudinal (L) directions at ambient temperature.

Tensile tests were performed according to the EN ISO 527 standard. The specimens were 150 × 20 mm large with a gauge length of 110 mm. Test speed was

2 mm/min. Tensile strength (σ_m) and modulus of elasticity (E_m) were calculated from the load-elongation (F-Δl) response of the specimens. Three-point bending tests were performed according to the EN ISO 14125 standard. The specimens were 70 × 20 mm large with a span length of 48 mm. Flexural strength (σ_f) and modulus (E_f) were calculated from the results.

SEN-T (single-edge notched tensile) specimens were used for static fracture mechanical tests. The 110 × 30 mm large specimens had a 10 mm deep sharp slot on one side produced by saw and razor blade. The specimens were subjected to tension at a speed of 2 mm/min using a Zwick Z020 type universal testing machine. From the load-elongation (F-Δl) response of the SEN-T specimens the static fracture toughness (K_{ICS}) was determined by equations (1) and (2) [21]:

$$K_{ICS} = \frac{F_{max}}{B \cdot W} \cdot a^{1/2} \cdot f(a/W), \tag{1}$$

where F_{max} is the maximum force, B is the thickness and W is the width of the specimen, a is the length of slot, f is a geometrical coefficient of correction:

$$f(a/W) = 1.99 - 0.41(a/W) + 18.7(a/W)^2 - 38.48(a/W)^3 + 53.85(a/W)^4. \tag{2}$$

Dynamic mechanical tests included Charpy and falling weight tests. The aim was to determine the energy absorption ability of composites, which is a very important factor for engineering applications.

Charpy tests were performed on a CEAST Resil Impactor instrument using a hammer with 15 J energy and 3.3 m/s speed according to the ISO 179 standard. The dimensions of specimens were 100 × 20 mm with a 5 mm deep sharp notch. Span length was 80 mm. Dynamic fracture toughness (K_{ICD}) was calculated from the results according to equations (3) and (4) [21], where a is the depth of notch and $\alpha = a/W$:

$$K_{ICD} = \frac{F_{max}}{B \cdot W} \cdot a^{1/2} \cdot f(a/W), \tag{3}$$

$$f(a/W) = 6\alpha^{1/2} \frac{[1.99 - \alpha(1-\alpha) \cdot (2.15 - 3.93\alpha + 2.7\alpha^2)]}{(1+2\alpha) \cdot (1-\alpha)^{3/2}}. \tag{4}$$

Falling weight tests were performed with a CEAST Fractovis 6785 instrument. Specimens were gripped in a pneumatic clamp with a 40 mm diameter hole. The size of the specimens was 60 × 60 mm. The falling dart had a hemispherical tip and a diameter of 20 mm. The mass of the falling weight was 8.26 kg and its speed was 5 m/s. The perforation energy (E_P) was calculated from the tests results by equation (5) [22]:

$$E_p = \frac{E_{max}}{B}, \tag{5}$$

Table 1.
Properties of the applied blown short (BF-B) and spun continuous (BF-S) basalt fibers compared with continuous glass fiber (GF)

Value marking	Diameter D_{av} (μm)	Cross section A_f (μm^2)	Maximum force F_{fs} (N)	Extension at failure Δl_{fs} (mm)	Tensile strength σ_{fs} (MPa)	Specific elongation ε_{fs} (%)	Elastic modulus E_f (GPa)
BF-B	9.0 ± 2.7	63.6 ± 40.4	0.03 ± 0.02	0.11 ± 0.04	419 ± 113	1.1 ± 0.4	60.4 ± 18.9
BF-S	14.2 ± 1.4	160.2 ± 30.3	0.32 ± 0.09	0.89 ± 0.22	2016 ± 434	3.6 ± 0.9	61.9 ± 3.5
GF	16.8 ± 1.6	223.4 ± 42.0	0.32 ± 0.08	0.68 ± 0.22	1472 ± 395	2.7 ± 0.9	57.0 ± 3.0

where E_{max} is the energy dissipated by the specimen and B is the thickness of the specimen. Similarly to static tests, dynamic tests also were performed at ambient temperature, using 5 specimens for each test.

3. RESULTS AND DISCUSSION

The properties of investigated fibers can be seen in Table 1. From the results it can be concluded that continuous basalt fiber (FB-S) has very good mechanical properties. Its tensile strength is higher than that of glass fiber by 40%. The modulus of elasticity of different fibers has approximately the same value. Short basalt fibers (BF-B) are considerably weaker than BF-S and glass fibers. BF-B fibers have relatively small diameter with high standard deviation; this derives from their production technology. During fiber formation BF-B fibers are exposed to different circumstances and cooling rates, so their structure contains numerous flaws, their diameter and length varies between wide boundaries and most of them contain so-called fiber heads (spherical objects) on fiber ends, which influence composite properties unfavorably [11]. Figure 2 shows an optical micrograph of blown basalt fibers made by Olympus BX51 microscope.

PP, BF-B and glass fibers were produced without coating. In order to produce an appropriate fiber–matrix interface we needed to be sure of the purity of fiber surfaces. Raman spectroscopy was used for this purpose. A LabRam instrument made by Jobin Yvon was used for our investigations, which is a dispersion Raman spectroscope combined with an Olympus optical microscope, which can identify the chemical composition of the sample surface. A Nd-YAG laser with a wavelength of 532 nm was used for our investigations. The chemical composition of the fiber surface was determined by spectra acquired in different depths from the surface. The confocal arrangement of the microscope supported the accuracy of depth measurements.

GF, PP and BF-B fibers showed the lack of surface treatment. On the other hand, glass fibers had differences in composition, depending on the depth. Figure 4 shows Raman spectra measured at 1, 0.5 and 0.1 μm depth from the fiber surface. Peaks around 2500 cm^{-1} can be associated with phosphorus compounds which are added

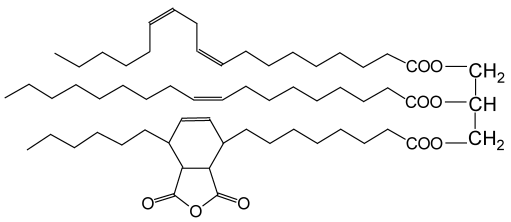

Figure 4. Schematic formula of NFO-MA adduct.

Table 2.
Static mechanical properties of investigated composites (σ_m: tensile strength, E_m: elastic modulus, σ_f: flexural strength, E_f: flexural modulus, K_{ICS}: static fracture toughness)

Mark of sample	σ_m (MPa)	E_m (GPa)	σ_f (MPa)	E_f (GPa)	K_{ICS} (MPa m$^{1/2}$)
PP	28.6 ± 0.3	1.3 ± 0.1	38.2 ± 1.0	1.5 ± 0.1	4.3 ± 0.2
BF-B L	30.8 ± 0.7	1.9 ± 0.1	51.7 ± 3.4	2.5 ± 0.3	5.2 ± 0.1
BF-B T	28.5 ± 0.6	1.8 ± 0.1	49.0 ± 3.2	2.3 ± 0.2	5.1 ± 0.1
GF L	98.4 ± 6.2	4.6 ± 0.2	133.4 ± 6.4	4.2 ± 0.3	11.5 ± 0.5
GF T	44.5 ± 1.9	2.4 ± 0.1	67.1 ± 3.0	2.8 ± 0.3	6.6 ± 0.2
BF-S L	47.4 ± 5.1	5.3 ± 1.3	150.0 ± 13.9	6.6 ± 0.2	12.1 ± 0.7
BF-S T	39.9 ± 3.4	3.2 ± 0.8	104.0 ± 3.8	4.3 ± 0.6	8.3 ± 0.8

Table 3.
Dynamic mechanical properties of investigated composites (K_{ICD}: dynamic fracture toughness, E_P: perforation energy)

Mark of sample	K_{ICD} (MPa m$^{1/2}$)	E_P (J/mm)
PP	1.9 ± 0.1	0.9 ± 0.1
BF-B L	3.1 ± 0.2	2.4 ± 0.3
BF-B T	2.8 ± 0.2	
GF L	12.2 ± 0.5	7.7 ± 0.7
GF T	7.1 ± 0.8	
BF-S L	6.9 ± 0.4	11.6 ± 1.8
BF-S T	5.2 ± 0.6	

to glass fibers as an additive. These compounds presumably accumulate in the middle of fibers during solidification; thus phosphorus content decreases near to the fiber surface. This phenomenon has a favorable effect on fiber strength, because phosphorus compounds have a strength decreasing effect on the surface [23].

Tables 2 and 3 show the results of composite mechanical tests. Directions L and T are differentiated according to the relative position of the fiber and notch (Fig. 5). Symbol L means that the direction of fibers is perpendicular to the notch and parallel to the direction of loading, while symbol T indicates that the fibers are parallel to the notch and perpendicular to loading.

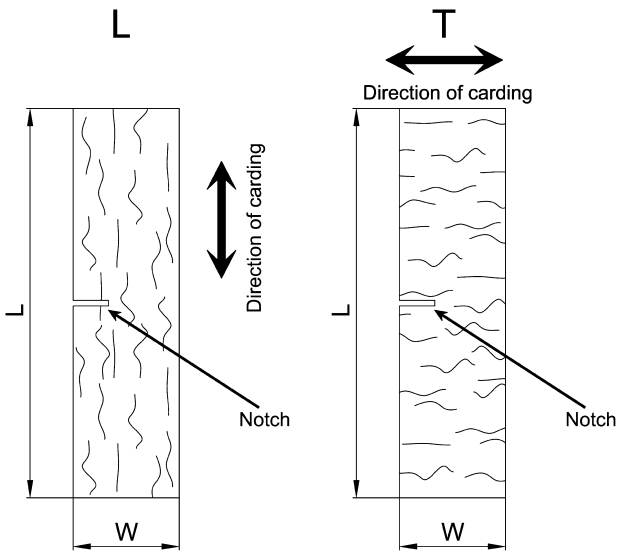

Figure 5. Schema of SEN-T and Charpy specimens cut in parallel (T) and perpendicular (L) to direction of carding.

The tensile strength and modulus of elasticity are not improved significantly by BF-B fiber reinforcement. Due to the better mechanical performance of the fiber, GF reinforced composites have better tensile properties. On the other hand, BF-S fibers give smaller tensile strength gain than GF, probably because of their weak adhesion to PP matrix. The flexural strength of BF-S fiber reinforced composites is higher than GF, in contrast with tensile properties. The reinforcing effect of BF-B is much more obvious in the case of bending. BF-B fibers improve the static fracture toughness only to a very small degree. Glass and BF-S fibers raise the value of K_{ICS} to a high degree. BF-S fiber reinforced composites have higher K_{ICS} than GF reinforced ones. Dynamic fracture toughness shows a similar trend: BF-B has only a small effect on this parameter, but BF-S and glass fibers reinforcement result in a tougher composite. Even BF-B fibers cause a large growth in perforation energy, although glass and BF-S fibers provide an even larger growth.

Figure 6 shows the scanning electron micrographs of fracture surface of a blown and a spun basalt fiber reinforced composite. BF-B fiber reinforced composites have much stronger adhesion between the fiber and the matrix, because they were treated with NFO-MA (Fig. 6(a)). On the other hand, BF-S fibers were treated with silane coupling agent optimized for epoxy resin; hence they adhere poorly to the non-polar PP matrix (Fig. 6(b)). Nevertheless, BF-S fiber reinforced composites had stronger mechanical properties, due to the superior performance of BF-S fibers.

4. CONCLUSIONS

Basalt fibers can be divided into two groups: continuous (spun) basalt fibers are produced by spinneret method, while short (blown) basalt fibers are prepared by

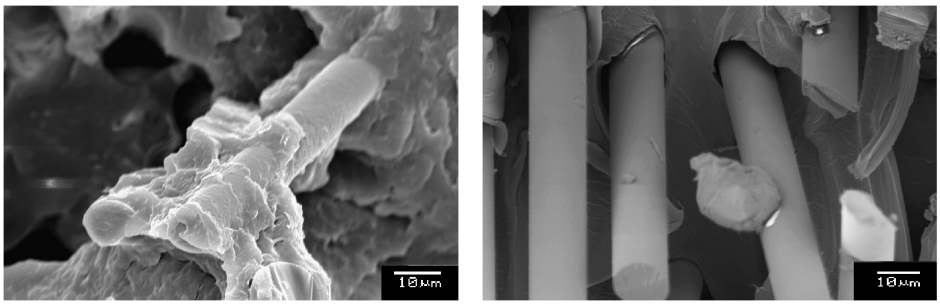

(a) (b)

Figure 6. Blown short (a) and spun continuous (b) basalt fiber reinforced PP composites.

melt blowing. Generally spun basalt fibers show better mechanical performance, but they are more expensive. The aim of this study was to compare different basalt and glass fibers and their PP matrix composites. The applied producing technology was carding, needle punching and hot pressing. These investigations were complemented with glass fibers. Spun basalt fibers (BF-S) have uniform geometrical and mechanical properties with an average diameter of 14 μm and a tensile strength over 2000 MPa. Blown basalt fibers (BF-B) feature fiber heads and short fibers with different length and varying diameter. The tensile strength of BF-B fibers is 5 times smaller than that of BF-S fibers. BF-B and glass fibers were compatibilized with the Diels-Alder adduct of sunflower oil and maleic acid-anhydride (NFO-MA) while BF-S fibers had a silane coating. Despite the poor adhesion of silane coupling agent to the non-polar PP matrix, BF-S reinforced composites show better tensile and flexural properties than glass fiber and BF-B reinforced composites, due to the superior properties of spun basalt fibers. In contrast with this, the dynamic fracture toughness of glass fiber reinforced PP is higher than BF-S composites, due to better interfacial adhesion. Spun basalt fibers (similarly to glass fibers) are suitable for demanding applications in composites, while blown basalt fibers rather can function as fillers for higher stiffness.

Acknowledgements

Kamenny Vek (Russia) and Toplan Ltd. (Hungary) are kindly acknowledged for the provision of basalt fibers. This work was supported by Jedlik Ányos Programme of Ministry of Economy and Transport of Hungary (ENGPL_07), Hungarian Scientific Research Fund (OTKA K61424) and Hungarian-Czech Science and Technology Programme (TéT CZ-1/08).

REFERENCES

1. T. Czigány, Trends in fiber reinforcements — the future belongs to basalt fiber, *Express Polym. Lett.* **1**, 59 (2007).

2. J. Militky, V. Kovacic and J. Rubnerová, Influence of thermal treatment on tensile failure of basalt fibers, *Engng Fract. Mech.* **69**, 1025–1033 (2002).
3. J. Militky and V. Kovacic, Ultimate mechanical properties of basalt filaments, *Textile Res. J.* **66**, 225–229 (1996).
4. N. N. Morozov, V. S. Bakunov and E. N. Morozov, Materials based on basalt from the European north of Russia, *Glass and Ceramics* **58**, 100–104 (2001).
5. T. Jung and R. V. Subramanian, Strengthening of basalt fiber by alumina addition, *Scripta Metallurgica et Materialia* **28**, 527–532 (1993).
6. J. M. Park, W. G. Shin and D. J. Yoon, A study of interfacial aspects of epoxy-based composites reinforced with dual basalt and SiC fibers by means of the fragmentation and acoustic emission techniques, *Compos. Sci. Technol.* **59**, 355–370 (1999).
7. S. Keszei, S. Matkó, G. Bertalan, P. Anna, G. Marosi and A. Tóth, Progress in interface modifications: from compatibilization to adaptive and smart interphases, *Eur. Polym. J.* **41**, 697–705 (2005).
8. G. Marosi, A. Márton, I. Csontos, S. Matkó, A. Szép, P. Anna, G. Bertalan and É. Kiss, Reactive surfactants — new type of additive for multicomponent polymer systems, *Prog. Colloid Polym. Sci.* **125**, 189–193 (2004).
9. G. J. Wang, B. Hu and Y. Feng, Low velocity impact properties of 3D woven basalt/aramid hybrid composites, *Compos. Sci. Technol.* **68**, 444–450 (2008).
10. V. V. Gurev, E. I. Neproshin and G. E. Mostovoi, The effect of basalt fiber production technology on mechanical properties of fiber, *Glass and Ceramics* **58**, 62–65 (2001).
11. L. M. Vas, K. Pölöskei, D. Felhős, T. Deák and T. Czigány, Theoretical and experimental study of the effect of fiber heads on the mechanical properties of non-continuous basalt fiber reinforced composites, *Express Polym. Lett.* **1**, 109–121 (2007).
12. T. Czigány, Discontinuous basalt fiber-reinforced hybrid polymer composites, in: *Polymer Composites: From Nano to Macro-Scale*, K. Friedrich (Ed.), pp. 309–328. Springer Verlag, München, Germany (2005).
13. Q. Liu, M. T. Shaw and R. S. Parnas, Investigation of basalt fiber composite mechanical properties for applications in transportation, *Polym. Compos.* **27**, 41–48 (2006).
14. F. Fourné, *Synthetic Fibers*. Carl Hanser Verlag, München, Germany (1999).
15. J. Sim, C. Park and D. Y. Moon, Characteristics of basalt fiber as a strengthening material for concrete structures, *Composites Part B* **36**, 504–512 (2005).
16. M. Botev, A. Betchev and D. Bikiaris, Mechanical properties and viscoelastic bahavior of basalt fiber reinforced polypropylene, *J. Appl. Polym. Sci.* **74**, 523–531 (1999).
17. J. S. Szabó and T. Czigány, Static fracture and failure behavior of aligned discontinuous mineral fiber reinforced polypropylene composites, *Polymer Testing* **22**, 711–719 (2003).
18. P. I. Bashtannik, A. I. Kabak and Y. Y. Yakovchuk, The effect of adhesion interaction on the mechanical properties of thermoplastic basalt plastics, *Mech. Compos. Mater.* **39**, 85–88 (2003).
19. T. Czigány, K. Pölöskei and J. Karger-Kocsis, Fracture and failure behavior of basalt fiber mat-reinforced vinylester/epoxy hybrid resins as a function of resin composition and fiber surface treatment, *J. Mater. Sci.* **40**, 5609–5618 (2005).
20. T. Czigány, Special manufacturing and characteristics of basalt fiber reinforced polypropylene composites: mechanical properties and acoustic emission study, *Compos. Sci. Technol.* **66**, 3210–3220 (2006).
21. J. G. Williams, *Fracture Mechanics of Polymers*. Ellis Horwood, New York, USA (1987).
22. T. M. Liu and W. E. Baker, Instrumented dart impact evaluation of linear low density polyethylene at controlled impact energy, *Polym. Engng Sci.* **31**, 753–763 (1991).
23. M. B. Volf, *Chemical Approach of Glass*. Elsevier, New York, USA (1984).